

# Elastic interaction between screw dislocations and a circular surface crack

K.M. Lin <sup>a,\*</sup>, H.C. Lin <sup>a</sup>, K.C. Chen <sup>a</sup>, H.L. Chang <sup>b</sup>

<sup>a</sup> Department of Materials Science, Feng Chia University, Taichung, Taiwan, ROC

<sup>b</sup> Institute of Materials Science and Engineering, National Chiao Tung University, Hsinchu, Taiwan, ROC

Received 5 September 1996

## Abstract

The behaviour of a screw dislocation around a circular surface crack was analyzed using the conformal mapping method. The effects of the crack length  $l$  and its radius of curvature  $R$  on the shielding effect and the strain energy were discussed in detail. It was found that for a dislocation being fixed at a constant distance from the crack tip and located on a plane tangent to crack surface at the tip, there exists a critical crack length  $l^*$  corresponding to a maximum shielding effect induced by the dislocation on the circular surface crack. The  $l^*$  increases with  $R$  and approaches infinity as the crack becomes planar (i.e.  $R \rightarrow \infty$ ). The shielding effect vanishes as the crack disappears. It increases rapidly with  $l$  if  $0 < l \ll l^*$ , regardless of  $R$ . After reaching the maximum, it decreases slightly for larger  $R$  but significantly for smaller  $R$  as the crack becomes longer. The shielding is more pronounced for larger  $R$  than that for smaller  $R$ , with the difference increasing with crack length. As a result, a surface microcrack propagates initially in a rather brittle manner then becomes more ductile. When the crack gets longer, it still keeps ductile for a less curved or a planar crack but becomes relatively brittle for a severely curved crack. In addition, the strain energy is also significantly influenced by crack length and increases rapidly with  $l$  when  $l$  is rather small, regardless of  $R$ . With increasing  $l$ , it becomes less affected by  $l$ , and the variation with  $R$  is still not obvious, with larger  $R$  corresponding to a slightly higher strain energy. © 1997 Elsevier Science S.A.

*Keywords:* Screw dislocations; Circular surface cracks; Elastic interaction; Conformal mapping method

## 1. Introduction

It is generally recognized that the process of the fracture in metals consists of three steps: (1) plastic deformation to produce dislocation pile-up; (2) the buildup of shear stress at the head of the pile-up to nucleate a microcrack; and (3) the stored elastic strain energy drives the microcrack to propagate associated with the dislocation emission from the crack tip to form a plastic zone. The fact that tensile stresses are not involved in the microcrack nucleation process but needed to make the microcrack propagate leads to the conclusion that crack propagation is ordinarily more difficult than crack initiation, and the fracture of metals is predominated by the process of crack propagation. Therefore, the ductility of metals is closely related to the behaviour of dislocations in the vicinity of the crack

tip, and the elastic interaction between dislocations and cracks has been paid much attention. For instance, using dislocation modelling, Louat [1] obtained the stress field around an internal crack and the image force on a screw dislocation. Majumdar and Burns [2] investigated an elastic theory of dislocations and dislocation arrays near a sharp crack. They proved that a screw dislocation always shields the crack from a mode III fracture. By analysing the ductile versus brittle behaviour of crystals, Rice and Thomson [3] proposed a dislocation emission criterion from a sharp crack tip. Using a planar distribution of continuous dislocations to simulate the plastic zone ahead of crack tips, Bilby et al. [4] predicted that the dislocations are inversely piled-up in the plastic zone. An in situ observation of the dislocation emission from a crack tip was carried out by Ohr [5] using transmission electron microscopy. He found that there exists a dislocation-free zone between crack tip and plastic zone. Following the Rice-Thom-

\* Corresponding author.

son model [3], Chang and Ohr [6] overcame the difficulty in the BCS theory [4] and established a dislocation-free zone model of fracture, which agrees with the observations in Ref. [5]. In addition, the interactions of dislocations with various types of cracks [7–13] were studied by using conformal mapping technique, dislocation modelling method and thermodynamic approach. Recently, the screw dislocations around a radial surface crack in a circular bar [14] and extended dislocations around a semi-infinite crack [15] have been investigated. These works were mainly focused on the dislocations interacting with a planar crack.

However, at elevated temperatures, a surface microcrack can be induced at the grain boundaries by environmental attack (e.g. oxidation or corrosion). Then it propagates along the grain boundaries under the action of an applied stress. Under such circumstances, the surface crack is not necessarily planar but becomes curved. Consequently, the dislocation–curved crack interaction is also significant. It prompted us to conduct this study. In the following, the crack geometry is taken to be circular, for simplicity, with the crack length and its radius of curvature as parameters. Attention is focused on the effects of crack geometry on the stress intensity factor and the strain energy. Finally, we summarize and present our conclusions.

## 2. Analysis and results

The dislocation–crack system we analyzed is shown schematically in Fig. 2(a). A semi-infinite medium with a free surface on the  $x$ -axis of the coordinate system is located on the upper half-space in the complex  $Z$ -plane. A circular surface crack emanating from the free surface is measured by the radius of curvature  $R$  and the central angle  $\alpha$ , so that its length yields  $l = R\alpha$ . A screw dislocation with Burgers vector  $\bar{b}$  around the crack tip is situated at the position  $Z_0 (= x_0 + iy_0)$ . Then, the elastic interaction between dislocation and crack can be investigated as follows.

### 2.1. Complex potential and stress field

Using a conformal mapping method, the interaction system can be transformed into an upper half-space in the complex  $\omega$ -plane with a screw dislocation located at  $\omega_0 (= u_0 + iv_0)$ , as shown in Fig. 2(b). The mapping function which relates  $\omega (= u + iv)$  to  $Z (= x + iy)$  is obtained as

$$\omega(Z) = R \left[ \left( \frac{Z - R}{Z + R} \right)^2 + \tan^2 \left( \frac{\alpha}{2} \right) \right]^{1/2} \quad (1)$$

The potential function of a screw dislocation in Fig. 2(b) is easily obtained by an image technique to yield

$$f(\omega) = \frac{b}{2\pi} \ln \left( \frac{\omega - \omega_0}{\omega - \bar{\omega}_0} \right) \quad (2)$$

with  $\bar{\omega}_0$  being the complex conjugate of  $\omega_0$ . Then substituting Eq. (1) into Eq. (2), we obtain the complex potential of the dislocation–crack system as

$$g(Z) = f[\omega(Z)] = \frac{b}{2\pi} \ln \left( \frac{D - D_0}{D - \bar{D}_0} \right), \quad (3)$$

where

$$D = \left[ \left( \frac{Z - R}{Z + R} \right)^2 + \tan^2 \left( \frac{\alpha}{2} \right) \right]^{1/2}, \quad (4a)$$

$$D_0 = \left[ \left( \frac{Z_0 - R}{Z_0 + R} \right)^2 + \tan^2 \left( \frac{\alpha}{2} \right) \right]^{1/2}, \quad (4b)$$

$$\bar{D}_0 = \left[ \left( \frac{\bar{Z}_0 - R}{\bar{Z}_0 + R} \right)^2 + \tan^2 \left( \frac{\alpha}{2} \right) \right]^{1/2}, \quad (4c)$$

and  $\bar{Z}_0$  denotes the complex conjugate of  $Z_0$ .

The stress field around the crack which arises from the screw dislocation is related to the complex potential by the following equation

$$\sigma_{yz} + i\sigma_{xz} = \mu g'(Z), \quad (5)$$

where  $\mu$  is the elastic shear modulus, and  $g'(Z)$  stands for the derivative of  $g(Z)$  with respect to  $Z$ . The subscript  $z$  denotes a coordinate direction. Substituting Eq. (3) into Eq. (5) and after tedious calculation, one obtains the stress components as

$$\sigma_{yz} = \frac{2\mu b R \rho^* r_0 \sin \theta_0 N}{\pi \rho^3 M^2 + N^2} \quad (6a)$$

and

$$\sigma_{xz} = \frac{2\mu b R \rho^* r_0 \sin \theta_0 M}{\pi \rho^3 M^2 + N^2}, \quad (6b)$$

where

$$M + iN = \exp[i(3\phi - \phi^*)] \left[ r^3 \exp(i3\theta) - 2r^2 r_0 \cos \theta_0 \exp(i2\theta) + r r_0^2 \exp(i\theta) \right], \quad (7a)$$

$$\rho^* \exp(i\phi^*) = Z - R, \quad (7b)$$

$$\rho \exp(i\phi) = Z + R, \quad (7c)$$

$$r \exp(i\theta) = D = \left\{ \left( \frac{\rho^*}{\rho} \right)^2 \exp[i2(\phi^* - \phi)] + \tan^2 \left( \frac{\alpha}{2} \right) \right\}^{1/2}, \quad (7d)$$

and

$$r_0 \exp(i\theta_0) = D_0 = \left\{ \left( \frac{\rho_0^*}{\rho_0} \right)^2 \exp[i2(\phi_0^* - \phi_0)] + \tan^2 \left( \frac{\alpha}{2} \right) \right\}^{1/2}. \quad (7e)$$

The variables  $\rho_0^*$ ,  $\phi_0^*$  and  $\rho_0$ ,  $\phi_0$  have the same definitions as  $\rho^*$ ,  $\phi^*$  and  $\rho$ ,  $\phi$  correspondingly with the

exception of  $Z$  in Eqs. (7b) and (7c) replaced by  $Z_0$ . Notice that  $M$ ,  $N$ ,  $r$  and  $r_0$  are dimensionless. Using numerical analysis, one proves that Eqs. (6a) and (6b) satisfy the boundary conditions, i.e.,  $\sigma_{yz}$  vanishes for  $y=0$  and  $\sigma_{tz}=0$  for  $Z=R \exp(i\beta)$ , where  $0 \leq \beta \leq \alpha$  and  $\sigma_{tz}$  denotes the shear stress acting on a plane tangent to the crack surface along the  $z$  direction.  $\sigma_{yz}$  and  $\sigma_{xz}$  are closely related to  $l$  and  $R$ . For a given crack length  $l$ , if  $R$  becomes infinite (so that  $\alpha$  approaches zero but  $R\alpha = l$  remains constant), it reduces to the case of a screw dislocation around a planar surface crack. Then Eqs. (6a) and (6b) are in agreement with the results obtained by Chu [7] and Juang and Lee [8].

## 2.2. Stress intensity factor

For a screw dislocation near a circular surface crack, the stress intensity factor at crack tip can be obtained by the relationship

$$K = \lim \{ -\sqrt{2\pi[Z - R \exp(i\alpha)]} (\sigma_{xz} \cos \alpha + \sigma_{yz} \sin \alpha) \} \quad (8)$$

as  $Z$  approaches  $R \exp(i\alpha)$ . Substituting Eqs. (6a) and (6b) into the above equation yields

$$K = -\frac{\mu b}{4\sqrt{\pi R}} \frac{\sin \theta_0}{r_0} \sqrt{\tan\left(\frac{\alpha}{2}\right)} 4 \frac{(1 + \cos \alpha - \sin \alpha)}{\cos^2\left(\frac{\alpha}{2}\right)}. \quad (9)$$

$K$  depends on the dislocation position  $(x_0, y_0)$  and is closely related to  $l$  and  $R$ . For a given crack geometry, its value is negative regardless of  $(x_0, y_0)$ . It implies that a screw dislocation always shields the tip of a circular surface crack from fracture. The shielding effect becomes more pronounced as the dislocation comes nearer the crack tip.

If the screw dislocation remains at a constant distance from the crack tip, the dependence of the shielding effect on crack geometry is illustrated in Fig. 1, where the stress intensity factor versus the crack length is plotted with the parameter  $R$  under the conditions  $d/a_0 = 40$  and  $\psi = \pi/2 + \alpha$ . The core radius of the dislocation is  $a_0$ . Both  $d$  and  $\psi$  denoting the dislocation position with respect to crack tip are defined by the equation

$$d \exp(i\psi) = Z_0 - R \exp(i\alpha). \quad (10)$$

That is, the dislocation is fixed at a distance  $d$  from the crack tip and located on a plane tangent to the crack surface at the tip. Fig. 1 clearly indicates that for a given radius of curvature  $R$ , the absolute value of  $K$  increases rapidly from zero, reaches a maximum corresponding to a critical crack length  $l^*$ , and then decreases when the crack length  $l$  increases from zero. For a relatively short crack, there's practically no difference

in  $K$  for a smaller or larger  $R$ . However, as the crack gets longer, the variation of  $K$  due to  $R$  becomes more significant. With increasing  $l$  the magnitude of  $K$  decreases obviously for smaller  $R$  but only slightly for larger  $R$  if  $l > l^*$ . The critical crack length  $l^*$  at a given  $R$  also increases with  $R$ . In addition, the curve for larger  $R$  always lies above that for smaller  $R$ . If  $R$  approaches infinity, a curve which becomes an upper bound in Fig. 1 is obtained, and the magnitude of  $K$  increases monotonically with crack length  $l$ . This corresponds to the case of a planar surface crack, and the present result agrees with those in refs. [7] and [8]. Based upon the above analysis, one infers that under the action of an applied stress, the fracture of a microcrack emanating from a free surface is relatively brittle, regardless of the radius of curvature  $R$  (i.e. either planar or curved). It occurs because the shielding effect induced by the dislocation on the crack is rather small. As the crack propagates, the shielding gets more effective and reaches a maximum if  $l = l^*$ . Then the fracture becomes more ductile. For a relatively long crack (if  $l > l^*$ ), the fracture of the crack still remains ductile for larger  $R$  (e.g. for a planar crack), but it becomes relatively brittle for smaller  $R$  (e.g. for a curved crack) because of the obvious decreasing in the shielding of the dislocation. In short, as compared with a planar surface crack, the degradation in ductility becomes more significant while the crack gets more curved.

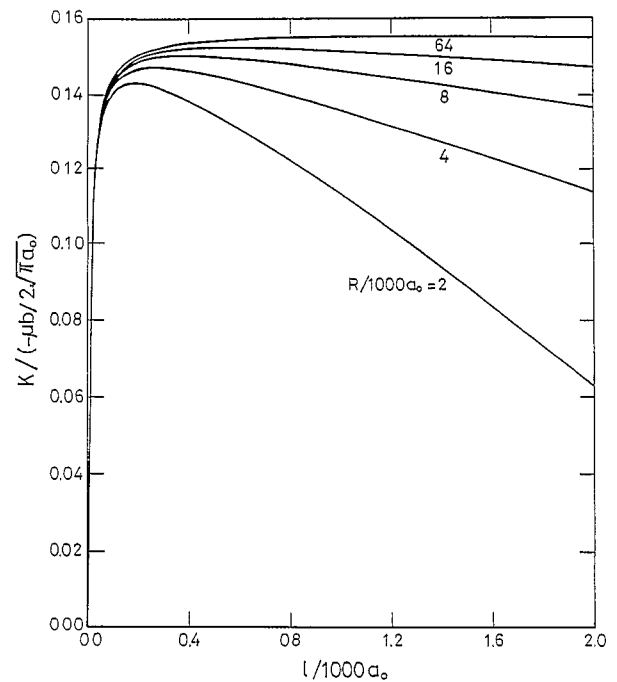


Fig. 1. The curves of the stress intensity factor as a function of crack length are plotted with  $R$  as a parameter under the conditions  $d/a_0 = 40$  and  $\psi = \pi/2 + \alpha$ , where  $d$  and  $\psi$  are defined in Eq. (10).

2.3. Strain energy and image force

Using Eqs. (6a) and (6b) and the imaginary cutting technique [8], the elastic strain energy of the screw dislocation per unit length is obtained as

$$E = \frac{\mu b^2}{4\pi} \ln\left(\frac{\rho_0^3 r_0^2 \sin \theta_0}{\rho_0^* a_0 R}\right). \tag{11}$$

Then, the image force on the dislocation can be obtained through  $F_x = -\partial E/\partial x_0$  and  $F_y = -\partial E/\partial y_0$ . Substituting Eq. (11) into these relationships, one obtains the force components as

$$F_x = -\frac{\mu b^2}{2\pi} \left\{ \frac{3 \cos \phi_0}{2\rho_0} - \frac{\cos \phi_0^*}{2\rho_0^*} + \frac{R\rho_0^*}{r_0^2 \rho_0^3} \left[ \cos(2\theta_0 + 3\phi_0 - \phi_0^*) + \frac{\sin(\phi_0^* - 3\phi_0 - \theta_0)}{\sin \theta_0} \right] \right\} \tag{12a}$$

and

$$F_y = -\frac{\mu b^2}{2\pi} \left\{ \frac{3 \sin \phi_0}{2\rho_0} - \frac{\sin \phi_0^*}{2\rho_0^*} + \frac{R\rho_0^*}{r_0^2 \rho_0^3} \left[ \sin(2\theta_0 + 3\phi_0 - \phi_0^*) + \frac{\cos(\phi_0^* - 3\phi_0 - \theta_0)}{\sin \theta_0} \right] \right\}. \tag{12b}$$

Note that by subtracting the self-stress components of the screw dislocation from Eqs. (6a) and (6b) respectively, it yields the image stress components on the dislocation. Then, substituting them into the Peach–Koehler equation, the same result as Eqs. (12a) and (12b) can also be obtained.

Eq. (11) indicates that the elastic strain energy is a function of the dislocation position  $(x_0, y_0)$  and closely related to the crack length  $l$  and its radius of curvature  $R$ . For any  $(x_0, y_0)$ ,  $l$  and  $R$ , the strain energy of the dislocation is always positive. However, its magnitude is strongly influenced by these parameters. Fig. 2 shows an example of the effect of crack geometry on the strain energy, where the strain energy  $E$  as a function of crack length  $l$  is represented with the radius of curvature  $R$  as a parameter under the same conditions as those in Fig. 1, i.e.  $d/a_0 = 40$  and  $\psi = \pi/2 + \alpha$  so that the screw dislocation keeps at a constant distance  $d$  from the crack tip on a plane tangent to crack surface at the tip. It indicates that for a screw dislocation with a distance  $d$  from a crack-free surface ( $l = 0$ ), the strain energy is approximately equal to 4.38 (in unit of  $\mu b^2/4\pi$ ). Once the microcrack is present, the strain energy is significantly affected by crack length if  $l < 250a_0$ . It increases rapidly with increasing  $l$ , regardless of the radius of curvature  $R$ . As the crack propagates ( $l > 250a_0$ ), the strain energy in-

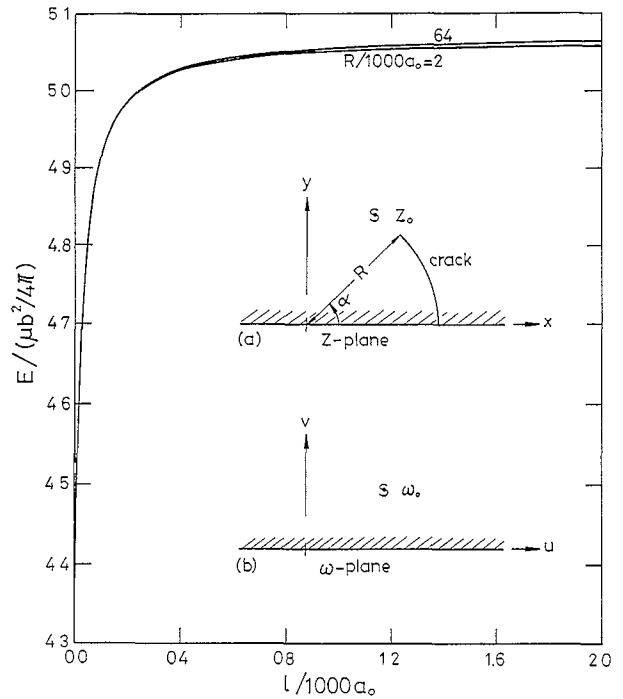


Fig. 2. The relationships of the strain energy versus crack length are represented with the parameter  $R$  under the same conditions as those in Fig. 1. Also shown in the inset is the schematic diagram of a screw dislocation (a) around a circular surface crack and (b) near a crack-free surface.

creases slowly and its value falls between  $E = 5.0$  and  $E = 5.1$ , with larger  $R$  corresponding to a larger value of  $E$ , but the difference in  $E$  for larger  $R$  and for smaller  $R$  is not obvious. For a finite crack length  $l$ , if  $R$  approaches infinity, Eq. (11) reduces to the results in Refs. [7] and [8]. It corresponds to the case of a screw dislocation near a planar surface crack. In addition, by comparing Fig. 2 with Fig. 1, it shows that for a relatively long crack, the dependence of the stress intensity factor  $K$  on the radius of curvature  $R$  is very pronounced, but it is not for the strain energy  $E$ . This occurs because the parameter  $R$  is contained in the logarithmic term in Eq. (11). Therefore,  $E$  becomes relatively insensitive to  $R$ .

The image force on the dislocation is also dependent on  $(x_0, y_0)$ ,  $l$  and  $R$ . With Eqs. (12a) and (12b), the trajectories of the screw dislocation around a circular surface crack can be obtained. The dislocation is attracted either by the free surface or by the circular surface depending on its initial position. Finally, if  $R$  becomes infinite but  $l$  remains finite with the screw dislocation near the crack tip, Eqs. (12a) and (12b) can be reduced to the result which agrees with those obtained by Chu [7] and Juang and Lee [8].

### 3. Summary and conclusions

The elastic interaction between a screw dislocation and a circular surface crack was investigated. The complex potential of the dislocation, the stress field around the crack, the stress intensity factor at crack tip, the strain energy of the dislocation and the image force on the dislocation were all derived. If the dislocation is fixed at a constant distance from crack tip and located on a plane tangent to crack surface at the tip, the shielding effect arising from the screw dislocation on a circular surface crack is strongly influenced by crack length  $l$  when the crack is relatively short. It vanishes for  $l=0$  and increases rapidly with increasing  $l$ , regardless of the radius of curvature  $R$  of the crack. After reaching a maximum which corresponds to a critical crack length  $l^*$ , the shielding effect decreases slightly for larger  $R$  but significantly for smaller  $R$  as the crack gets longer ( $l > l^*$ ). The  $l^*$  increases with  $R$ . For a finite crack that's not very short, the shielding effect is more pronounced for larger  $R$  than for smaller  $R$ , with the difference between them increasing with  $l$ . Consequently, during the propagation of a surface microcrack, it occurs first in a rather brittle form and then becomes relatively ductile. While the crack gets longer and longer, it still remains ductile for a planar or a less curved crack (i.e. for larger  $R$ ), but becomes relatively brittle for a severely curved crack (i.e. for smaller  $R$ ). In short, the ductility is decreased by increasing the curvature of the crack. In addition, for a given  $R$  with

increasing  $l$  from zero, the strain energy initially increases rapidly, showing the same trend as the shielding effect, and then slowly. As the crack gets longer, it becomes practically independent of  $l$ , with larger  $R$  corresponding to a higher strain energy. The variation with  $R$  is not obvious for the strain energy, which is significantly different from that for the shielding effect. Finally, the exact formulas of the physical variables derived in this paper can be reduced to the case of a planar surface crack. The results also agree with those in the literature.

### References

- [1] N.P. Louat, *Proc. 1st Int. Conf. Fracture, Sendai, 1965*, p. 117.
- [2] B.S. Majumdar and S.J. Burns, *Acta Metall.*, 29 (1981) 579.
- [3] J.R. Rice and R. Thomson, *Philos. Mag.*, 29 (1974) 73.
- [4] B.A. Bilby, A.H. Cottrell and K.H. Swinden, *Proc. R. Soc. London, Ser. A*, 272 (1963) 304.
- [5] S.M. Ohr, *Mater. Sci. Eng.*, 72 (1985) 1.
- [6] S.J. Chang and S.M. Ohr, *J. Appl. Phys.*, 52 (1981) 7174.
- [7] S.N.G. Chu, *J. Appl. Phys.*, 53 (1982) 8678.
- [8] R.R. Juang and S. Lee, *J. Appl. Phys.*, 59 (1986) 3421.
- [9] K.M. Lin, C.T. Hu and S. Lee, *J. Appl. Phys.*, 63 (1988) 726.
- [10] S.D. Wang and S. Lee, *Mater. Sci. Eng.*, A130 (1990) 1.
- [11] K.M. Lin, C.T. Hu and S. Lee, *Mater. Sci. Eng.*, 95 (1987) 167.
- [12] K.M. Lin, C.T. Hu and S. Lee, *Eng. Fract. Mech.*, 45 (1993) 321.
- [13] S.T. Shiue and S. Lee, *Eng. Fract. Mech.*, 22 (1985) 1105.
- [14] K.M. Lin and H.L. Chang, *Mater. Sci. Eng.*, A187 (1994) 139.
- [15] K.M. Lin, H.C. Lin and K.C. Chen, *Eng. Fract. Mech.*, 54 (1996) 395.